An Update on the Ice Climatology of the Hudson Bay System

Authors: Hochheim, Klaus P., and Barber, David G.

An Update on the Ice Climatology of the Hudson Bay System

Klaus P. Hochheim*† and
David G. Barber*‡

*Centre for Earth Observation Science
(CEOS), Clayton H. Riddell Faculty
of Environment, Earth, and Resources,
Wallace Building, University of
Manitoba, 125 Dysart Road, Winnipeg,
Manitoba, R3T 2N2, Canada
†Deceased
‡Corresponding author:
David.Barber@umanitoba.ca

Abstract

The objective of this paper is to examine the thermodynamic and dynamic forcing of sea ice within the Hudson Bay System, including Hudson Bay, Hudson Strait, and Foxe Basin. Changes in fall and spring sea ice extents (SIEs) are examined in relation to seasonal surface air temperatures (SATs) and winds, as are changes in freeze-up dates and breakup dates. The proportional leverage of the fall (lag1) and spring SATs and winds on ice is statistically examined per basin. Results show SATs have increased significantly since the mid-1990s and that increases in the fall are higher than the spring period. Fall SATs are highly related to fall SIEs ($R^2 = 0.79$–0.82). For every 1 °C increase in SAT, SIE decreases by 14% (% of basin area) within the Hudson Bay System; a 1 °C increase delays freeze-up by 0.7 to 0.9 weeks on average. Spring SIEs and breakup dates are shown to be highly correlated with fall (lag1) and spring SATs, and with U and V component winds. Proportionately, spring and fall SATs combined play a dominant role (70–80%) in SIE, and the remaining leverage is attributed to dynamic forcing (winds). The relative leverage of fall (lag1) SATs and surface winds are shown to be significant and vary by basin. The open water season has on average increased by 3.1 (±0.6) weeks in Hudson Bay, 4.9 (±0.8) weeks in Hudson Strait, and 3.5 (±0.9) weeks in Foxe Basin.

Introduction

This paper focuses on recent changes in interannual sea ice extent (SIE) and ice freeze-up/ice breakup dates within the subarctic region of eastern Canada, including Hudson Bay, Foxe Basin, and Hudson Strait, from 1980 to 2010. Changes in sea ice are examined as a function of dynamic and thermodynamic forcing.

Strong negative trends in SIE are a relatively recent phenomenon within the satellite record. Prior to the mid-1990s, much of eastern Canada, including Baffin Bay/Davis Strait and the Labrador Sea, showed a slight positive trend in SIE (2.0×10^4 km^2 year^{-1}), and the Hudson Bay region showed similar positive trends in SIE (Parkinson and Cavalieri, 1989; Deser and Teng, 2008). Positive trends in ice breakup date (later breakup) based on Canadian Ice Service (CIS) data (1971–1989) were also noted by Galbraith and Larouche (2011): +2.3 days decade^{-1} for Hudson Strait, 2.0 days decade^{-1} for Hudson Bay, and a weak negative trend (–0.9 days decade^{-1}) for Foxe Basin. These trends in SIE were also corroborated by Canadian Ice Service data from 1960–1990, which showed positive trends in ice thickness over this period (Gagnon and Gough, 2005).

Using CIS data from 1971–2003, Gagnon and Gough (2005) started to detect statistically significant negative trends in ice breakup date in western Hudson Bay, along the Hudson Bay south coast, and in James Bay, with trends ranging from –4.9 to –12.5 days decade^{-1}. Significantly later freeze-up dates in fall were confined to the northwestern portion of Hudson Bay (3.2–5.5 days decade^{-1}). Strong basinwide trends to earlier breakup within the Hudson Bay System (HBS) were detected from 1990 to 2009 (Galbraith and Larouche, 2011), particularly for Foxe Basin and Hudson Strait (–9 days and –13.5 days decade^{-1}, respectively), less so for Hudson Bay (–1.9 days decade^{-1}) where the longer term trend from 1971 to 2009 was more significant at –3.2 days decade^{-1}.

Variations in interannual SIE are closely tied to changes in seasonal SATs and winds in the Hudson region (Hochheim and Barber, 2010; Hochheim et al., 2011). In the mid-1990s, a notable shift to warmer seasonal surface air temperature (SAT) anomalies occurred during the fall (SON) and spring (AMJ) periods over the Hudson Bay region making the 1996–2005 period statistically unique from previous semi-decadal periods. Mean three-month seasonal SATs in the Hudson Bay area have increased by approximately 0.30 °C decade^{-1} (1960–2005) during the spring breakup (AMJ—April, May, June). SAT changes in the fall (SON—September, October, November) period have occurred more recently (1980–2005) where temperatures are trending slightly higher 0.70 °C decade^{-1} (Hochheim et al., 2011). Variability of climate over the HBS has been linked to various large-scale hemispheric-scale indices (Wang et al., 1994; Mysak et al., 1996; Prinsenberg et al., 1997; Qian et al., 2008; Hurrell et al., 2004, 2006; Kinnard et al., 2006; Hochheim and Barber, 2010).

The objectives of this paper are to provide an update to results of previous work as it relates to thermodynamic and dynamic forcing of sea ice over Hudson Bay, including Hudson Strait and Foxe Basin. An update will be provided for each region within the HBS in terms of (1) surface air temperature (SAT) trends, (2) seasonal trends in sea ice extent, (3) trends in breakup and freeze-up dates as a function of surface air temperature and winds, and (4) showing the spatial distribution of cumulative changes in the sea ice season for the HBS.

Methods

STUDY AREA

The study area comprises Hudson Bay (including James Bay), Foxe Basin, and Hudson Strait. These together are commonly referred to as the HBS (Saucier et al., 2004) (Fig. 1). The HBS is a large-scale estuarine system with a riverine input of ~900 km^3 year^{-1}, which it receives from much of western and northeastern Canada and represents 20% of the total annual runoff to the Arctic Ocean (Déry and Wood, 2004; Déry et al., 2005).
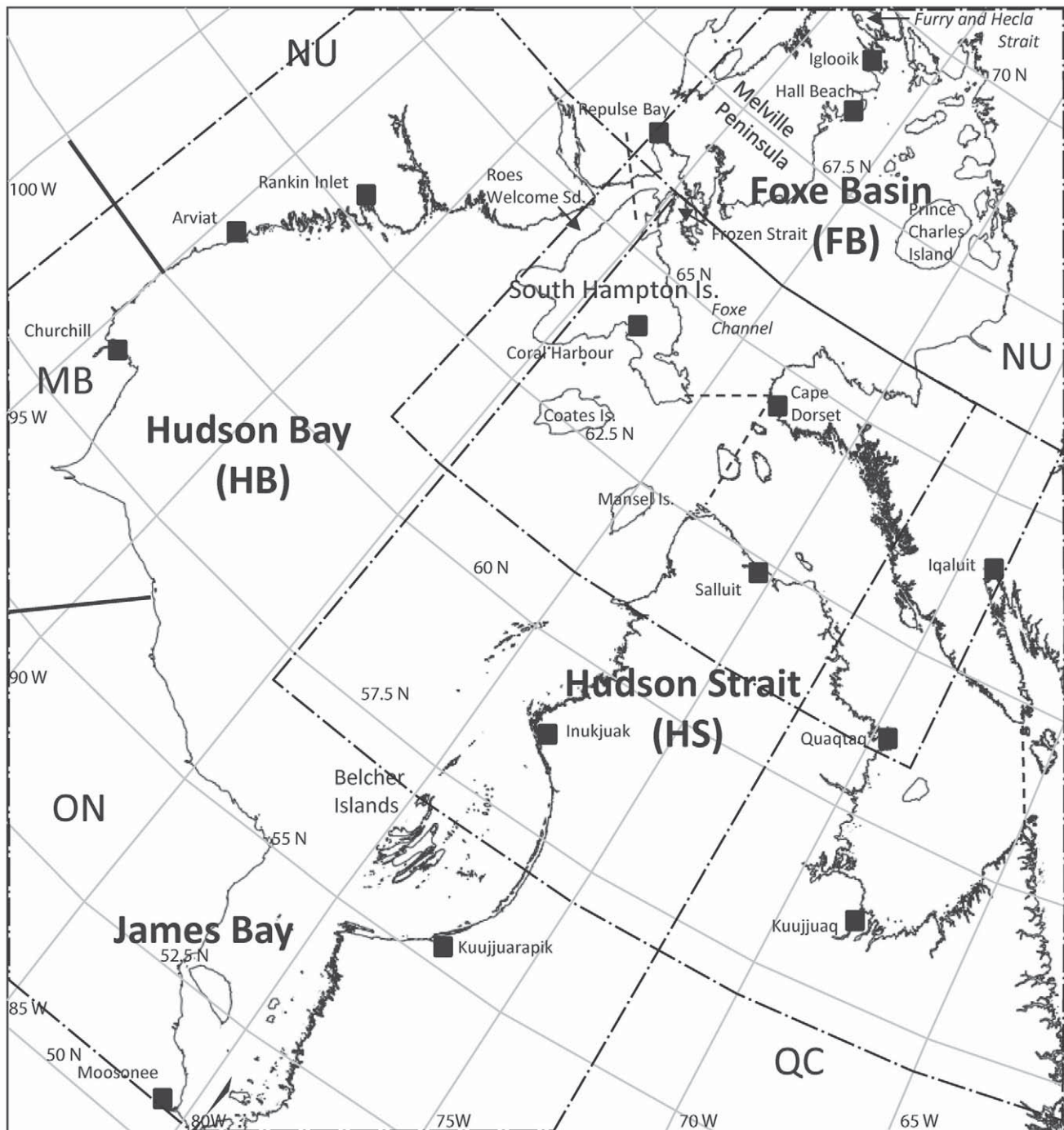
FIGURE 1. Map of the Hudson Bay System (HBS). Dot-dash lines show the bounds for temperature trend analysis in the individual subregions. Hudson Bay (HB), Hudson Strait (HS), and Foxe Basin (FB) are abbreviated in subsequent figures and tables.

Hudson Bay is relatively shallow (150 m mean depth) and connected to the Labrador Sea through Hudson Strait and the Arctic Ocean through Foxe Basin (Prinsenberg, 1986b). Shallow sills isolate Hudson Bay from open ocean circulation; therefore, variations in interannual sea ice cover are largely attributed to local atmospheric forcing (Etkin, 1991; Wang et al., 1994; Saucier and Dionne, 1998). Currents within Hudson Bay are predominantly wind driven and cyclonic at all depths, reaching a maximum in November (Saucier et al., 2004). The currents in James Bay are

also cyclonic, driven by a combination of winds and local runoff from major river systems entering the Bay. Sea ice generally starts to form along the northwestern coast of Hudson Bay and along Southampton Island starting early November and progresses southeastward; eastern James Bay and Hudson Bay are the last to freeze up (Hochheim and Barber, 2010). Maximum ice growth rates are found in northwestern Hudson Bay in a large, persistent polynya and in western Foxe Basin (Saucier et al., 2004), whereas ice growth in the western portion of the HBS is largely

KLAUS P. HOCHHEIM AND DAVID G. BARBER / 67

thermodynamic. Dynamic processes of advection and ridging are dominant factors contributing to ice thickness in the eastern portion of the basins (Saucier et al., 2004). Spring melt in Hudson Bay begins late May to early June along the coastal regions to the northwest and northeast as well as James Bay. Last remnants of ice are generally located along the southwestern coast of Hudson Bay because of currents and wind forcing. Hudson Bay is usually ice free in early August (Hochheim et al., 2011).

Foxe Basin has an area of ~207,500 km²; it is connected to Hudson Bay via Roes Welcome Sound, to Hudson Strait via Foxe Channel, and to the Arctic waters via Fury and Hecla Strait (Fig. 1). Ice within Foxe Basin is almost exclusively first-year ice with a small potential of remnant second-year ice in the fall. Ice transport in the central portion of the basin is largely wind driven (Prinsenberg, 1986a). A polynya occurs in the northwest portion of Foxe Basin along the west coast near Hall Beach. A combination of winds and currents moves the ice southward toward the Hudson Strait along the western coast of Foxe Basin. Late in the melt season, ice from Hudson Strait may be transported west into southern Foxe Basin by currents along the northern coast of Hudson Strait; late-season residual ice is often found off the northeast shore of South Hampton Island (Prinsenberg, 1986a, 1986b). Seasonal variations in ice cover are a function of SATs, and regional winds may enhance or inhibit ice export out of Foxe Basin. Historically, freeze-up typically starts 15–22 October and is fully ice covered by 12 November. Melt season generally starts around mid-June; by mid-September Foxe Basin is generally ice free.

Hudson Strait is a long (400 km) channel that connects the HBS to the Labrador Sea. It has an area of ~189,000 km², and a mean depth of 300 m. Currents along its northern coast flow into Hudson Strait from the Labrador Sea and drift northwesterly to the Foxe Channel and into northern Hudson Bay (St-Laurent et al., 2011). The currents along the southern coast of Hudson Strait flow southeasterly to the Labrador Sea (Sutherland et al., 2011). During the fall and winter the surface waters of Hudson Strait tend to be highly stratified as summer runoff and melt waters move through from Hudson Bay (Stewart and Barber, 2010; Sutherland et al., 2011).

Hudson Strait typically starts to freeze up around mid-November from the northwest and progresses to the southeast. Hudson Strait is typically ice covered by mid to late December. During the winter period, ice within the channel remains unconsolidated (Prinsenberg, 1986a) as a result of local currents and prevailing winds. Melt usually begins late May to early June. The first ice-free areas are typically along the northern coast of Hudson Strait (because of prevailing northwest winds) and south coast of Ungava Bay. Ice concentrations are highest along the southern half of the Hudson Strait channel during the breakup period. Hudson Strait is generally ice free by the end of July.

SEA ICE DATA

PMW Data

The sea ice concentration (SIC) data were obtained from passive microwave (PMW) data processed at the National Snow and Ice Data Center (NSIDC) (Comiso, 2000). The sea ice data are provided in a polar stereographic projection and have a spatial resolution of 25 km. Though it is known that PMW data may underestimate the absolute concentrations of sea ice marginal zones during freeze-up and melt-out conditions, it is the only internally consistent weekly data set available over the 31-year period for the HBS capturing both late freeze-up and early spring breakup

on a weekly basis. These data are used to examine interannual trends in SIE, freeze-up dates, and breakup dates as a function of thermodynamic and dynamic forcing.

Sea ice anomaly data are used to minimize bias of the SIE retrievals; these were computed using 1980–2010 weekly means as a baseline. SIE anomalies are based on percent coverage of the basins with SICs ≥ 60%, reflecting the interest in mapping trends of the more "consolidated ice." Freeze-up and breakup dates (anomalies) are defined by 50% cover of a basin with SICs ≥60%.

THERMODYNAMIC AND DYNAMIC FORCING OF SEA ICE

Surface Air Temperature

Surface air temperature data used to examine regional temperature trends surrounding the HBS were computed using CANGRID data (Environment Canada, 2013). These data are developed by the Climate Research Division of Environment Canada. It uses adjusted historical Canadian climate data that accounts for changes resulting from reporting-station system changes (Vincent and Gullett, 1999; Vincent et al., 2012). The CANGRID grid data have a spatial resolution of 50 km and cover land surfaces only. These data are selected in place of reanalysis data as there are very limited data available to assimilate into reanalysis for the study region during the full period of interest, making it difficult to ascertain their accuracy and homogeneity.

The CANGRID data include monthly mean air temperatures dating back to 1950, when most stations in the region were reporting on a regular basis. Regional temperature anomalies were computed relative to 1980–2010 temperature normals; these match the normals computed for the sea ice data. The use of temperature anomalies in gridding data has the advantage of removing location, physiographic, and elevation effects. A three-month running mean was applied to the monthly SAT anomaly data ending in (including) the month of interest; the intent here was to incorporate lead-up SATs to obtain a (moving) seasonal temperature index (anomaly) value. We tested both normality and autocorrelation (assumptions of the general linear model), and we found each to be sufficiently low to allow for use of parametric analysis. SAT anomaly trends and their statistical significance (p at 0.10, 0.05, and 0.01) were mapped based on the least-squares fit per grid point. Regional seasonal SATs were also examined on a basinwide scale using either linear or polynomial trends where appropriate. Examination of mean SATs at 15-year intervals over 1950–2010 was based on one-way analysis of variance (ANOVA); significance testing was based on either parametric tests (t-test or Tukey Krammer t-test) or non-parametric test (Wilcoxon). In this paper, parametric assumptions are implied unless otherwise specified.

These seasonal temperature data were used to (1) examine general regional trends of SATs in the fall and spring, (2) establish relationships between SAT anomalies and regional SIE anomalies, and (3) examine SAT anomalies in relation to freeze-up dates and breakup dates. Bounds used to compute mean SATs for Hudson Bay are 51.0064–65.9835N; 72.5161–97.464W; bounds for Hudson Strait are 57.0011–65.9779N, 63.0392–84.9535W; and for Foxe Basin 61.02–71.73N, 69.02–86.97W (Fig. 1).

Winds

Wind data were used to determine whether zonal (U) or meridional (V) winds at 1000 mb are predictive of interannual SIEs, particularly during spring breakup. Winds are based on NCEP_Reanalysis 2 data (NOAA Earth System Research

Laboratory, 2011). Seasonal three-month mean wind anomalies were computed using 1980–2010 as a baseline. Reanalysis data are used as there are no other sources of homogenized, spatially and temporally continuous data available for the region.

Within the HBS, both the Foxe Basin and Hudson Strait have an "outlet." The hypothesis is that the strong positive U component (westerly) wind over the Hudson Strait may enhance ice export in the spring melt period; alternatively, a strong negative component over the same area may inhibit ice export during the melt-out period and therefore contribute to a positive SIE anomaly. For the Foxe Basin region, variations in the V component of winds may be of interest; that is, a strong negative V component may imply greater ice export from the Foxe Basin via the Foxe Channel into Hudson Strait.

As shown in Hochheim et al. (2011), wind-forced ice vorticity in the spring significantly contributed in predicting SIE in Hudson Bay; positive ice vorticity in Hudson Bay was predictive of lower SIEs. The ice vorticity data set has not been updated to 2010; instead, we examine the U and V components of winds over western Hudson Bay.

Results

REGIONAL SAT TRENDS

The spatial distribution of seasonal surface air temperature (SAT) trends over 1980–2010 surrounding the HBS are shown in Figure 2. In the fall period, September to November (SON) temperature trends (β) are highest in northern reaches of Hudson Bay and areas surrounding Hudson Strait and Foxe Basin (0.8–1.1 °C decade^{-1}). Southern Hudson Bay temperature trends

range between 0.6 and 0.8 °C decade^{-1}. During the spring period (AMJ), when sea ice extent (SIE) anomalies exhibit the greatest interannual variation, the largest SAT trends appear to be centered over Hudson Strait and Foxe Basin and the northern and eastern regions of Hudson Bay. The SAT trends around Hudson Strait and Foxe Basin range from 0.7 to 0.9 °C decade^{-1}; trends surrounding Hudson Bay are more varied, with the highest temperature trends (0.5–0.9 decade^{-1}) occurring in the northern and eastern portions of the basin.

To put the spatially mapped SAT trends for the satellite period into context (Fig. 3, parts a–f) shows the seasonal SAT anomalies per region from 1950 to 2010 for fall and spring. The seasonal SATs chosen for each region/season were most predictive of regional SIE anomalies. Various spline fits were used to qualitatively highlight (1) the high interannual variations in SAT per season/region (l = 0.01), (2) the cyclical nature of temperatures (l = 0.25), and (3) the overall general trend (l = 827) in regional SAT anomalies. Quantitatively, linear or polynomial SAT trends (β) and their significance (p) for each basin are summarized in Table 1; these are computed for 1950–1979, 1980–2010, and 1950–2010.

During freeze-up, the longer-range temperature trends (1950–2010) are best characterized by a second-order polynomial and were all highly significant ($p = 0.01$ or 0.05) (Table 1 and Fig. 3, parts a, c, and e). The linear trends from 1950–1979 are all slightly negative but statistically nonsignificant. These negative trends reflect a brief global cooling period from about 1940 to 1970; hence the polynomial fits in the fall period over the HBS. The linear trends (β) from 1980–2010 are all significant at 99% probability; the mean regional SAT trend for Hudson Bay (SON) is approximately 0.8 °C decade^{-1}; the trend for Hudson Strait (OND)
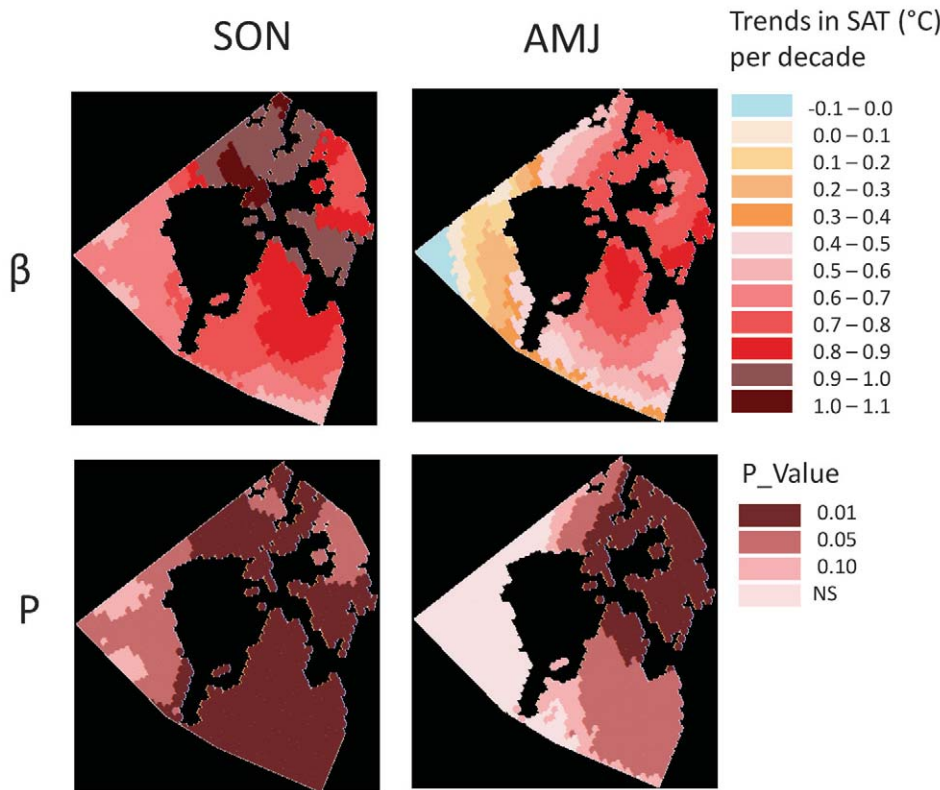
FIGURE 2. Mean seasonal surface air temperature (SAT) trends (β) per decade (1980–2010) including significance (p) at 99, 95, and 90% levels.

TABLE 1

Seasonal surface air temperature (SAT) anomaly trends (β) per year and their significance (p) per region for fall and spring. Months used to compute SAT trends per season/region are those most predictive of interannual sea ice extents (SIEs) (1980–2010).

Subarea (months)	Years	Fall				Subarea (Months)	Spring				N
		β1	β2	p1	p2		β1	β2	p1	p2	
HB	1950–2010	**0.0232**	**0.0015**	**0.0133**	**0.0147**	HB	~~0.0237~~	~~0.00071~~	~~0.0189~~	~~0.2539~~	61
(SON)	1950–1979	~~−0.0094~~		~~0.7256~~		(AMJ)	0.0082		0.762		30
	1980–2010	*0.0791*		0.004			~~0.0423~~		~~0.1589~~		31
HS	1950–2010	*0.0491*	*0.0026*	*0.0007*	*0.0039*	HS	~~0.0115~~	~~0.0023~~	~~0.2264~~	*0.003*	61
(OND)	1950–1979	~~−0.0151~~		~~0.6979~~		(AMJ)	-0.0491		0.0967		30
	1980–2010	*0.1509*		*0.0005*			*0.00815*		*0.0042*		31
FX	1950–2010	**0.0447**	**0.0017**	*0.0003*	**0.0258**	FX	**0.0207**	**0.0014**	**0.0178**	**0.0108**	61
(SON)	1950–1979	~~−0.0135~~		~~0.6927~~		(MJJ)	~~−0.0357~~		~~0.1896~~		30
	1980–2010	*0.0940*		*0.0063*			**0.0499**		**0.0312**		31

Bold Italic p = 0.01; **Bold p = 0.05**; plain text p = 0.10; strikethrough = NS.
HB = Hudson Bay, HS = Hudson Strait, FX = Foxe Basin, SON = September-October-November, OND = October-November-December, AMJ = April-May-June, MJJ = May-June-July.

is highest at 1.5 °C decade^{-1}; and for Foxe Basin (SON) the trend is 0.9 °C decade^{-1} (Table 1).

Mean SAT anomalies for the fall were conducted at 15-year intervals from 1950 to 2010, as identified in Figure 3 (parts a–f), using one-way analysis of variance (ANOVA). This interval captures the transition from the previous cooler regimes to the warmer regime starting around 1996 and extending to 2010 (Hochheim and Barber, 2010). The results indicate that 1996–2010 remains statistically warmer compared to all preceding 15-year intervals. Mean seasonal SAT differences (D) for each interval relative to 1996–2010 are highest in Hudson Strait, ranging from –2.67 to –2.89 °C, followed by Foxe Basin ranging from –1.85 to –2.34 °C and Hudson Bay where SAT differences range from –1.47 to –2.02 °C (Fig. 3, parts a, c, and e). Note that the very high SAT differences in Hudson Strait reflect an extraordinary temperature anomaly (5.8 °C) in the fall of 2010 resulting from a prolonged high-pressure anomaly over Greenland.

The Hudson Bay SAT anomalies in spring show considerable interannual variation, particularly over 1996–2010 (Fig. 3, part b). SAT's trend around Hudson Bay from 1950–1979 is slightly positive (0.082 °C decade^{-1}) but statistically nonsignificant, and the trend from 1980 to 2010 is much higher (0.42 °C decade^{-1}) but also nonsignificant (Table 1) because of the large interannual variability of the SATs and relatively small sample size. Extending the observations from 1960 to 2010, the trend becomes significant, 0.32 °C decade^{-1} ($p = 0.011$). The SAT anomalies at 15-year intervals during AMJ reveal that only 1950–1965 was for Hudson Bay statistically different from 1996–2010 at $p = 0.08$ (Wilcoxon Test).

For the Hudson Strait area, the spring SAT trend from 1980 to 2010 is estimated at 0.82 °C decade^{-1} ($p = 0.004$) (Table 1). The trend from 1950 to 1979 was negative at –0.49 °C decade^{-1} ($p = 0.097$). Examining the 15-year average seasonal SATs for Hudson Strait, the two intervals preceding 1996–2010 were significantly cooler, 1.42 to 1.61 °C (Fig. 3, part d).

For the Foxe Basin region, the long-term (1950–2010) spring SAT trend was best represented by a second-order polynomial fit (p

= 0.0108) with the hinge point around the mid-1970s. The seasonal linear SAT trend (MJJ—May, June, July) from 1950 to 1979 is –0.36 °C decade^{-1} although not significant; the trend from 1980 to 2010 is 0.50 °C decade^{-1} ($p = 0.0312$), lower than Hudson Strait but higher than the Hudson Bay SAT trend for the same period. Examining the mean SATs at the 15-year intervals, 1996–2010 was statistically warmer by 0.93 to 1.42 °C compared to all preceding intervals (Fig. 3, part f).

CHANGES IN SEA ICE EXTENT

Fall SIE

In the preceding section we showed that seasonal temperatures within the HBS have increased significantly since the mid-1990s in both the fall (1.5–2.9 °C) and spring (0.8–1.6 °C), depending on the region. Here we examine the relationship between observed mean three-month seasonal SATs and mean three-week SIEs (based on SIC ≥ 60%) for each of the regions within the HBS.

For the Hudson Bay region, SIE anomalies averaged over week of year (WOY) 47–49 (19 November–5 December) are best correlated to three-month seasonal SATs ending November (SON); $R^2 = 0.79$, $p < 0.001$ (Table 2 and Fig. 4, part a). Based on the regression estimates, for each 1 °C increase in the seasonal SAT, sea ice extent decreases by 14.4% or 1.34 × 10^5 km² (± 2.59 × 10^3 km²). The seasonal SAT anomaly range for the area surrounding Hudson Bay (1980–2010) for SON ranges from –3.5 to 2.1 °C, the resulting predicted SIEs ranging from 16% of Hudson Bay area (or 1.48 × 10^5 km²) to 97% (or 89.9 × 10^5 km²). To obtain an ice-free Hudson Bay during the WOY 47–49 requires a mean seasonal temperature anomaly of +3.2 °C and a –3.7 °C anomaly for complete cover. The mean difference in SIEs between 1980–1995 vs. 1996–2010 is 30.5% (±6.6%) or 2.83 × 10^5 km² (±6.1 × 10^4 km²) (Fig. 4, part b). The mean change in SIE is associated with mean increase of 1.5 °C (Fig. 3, part a).
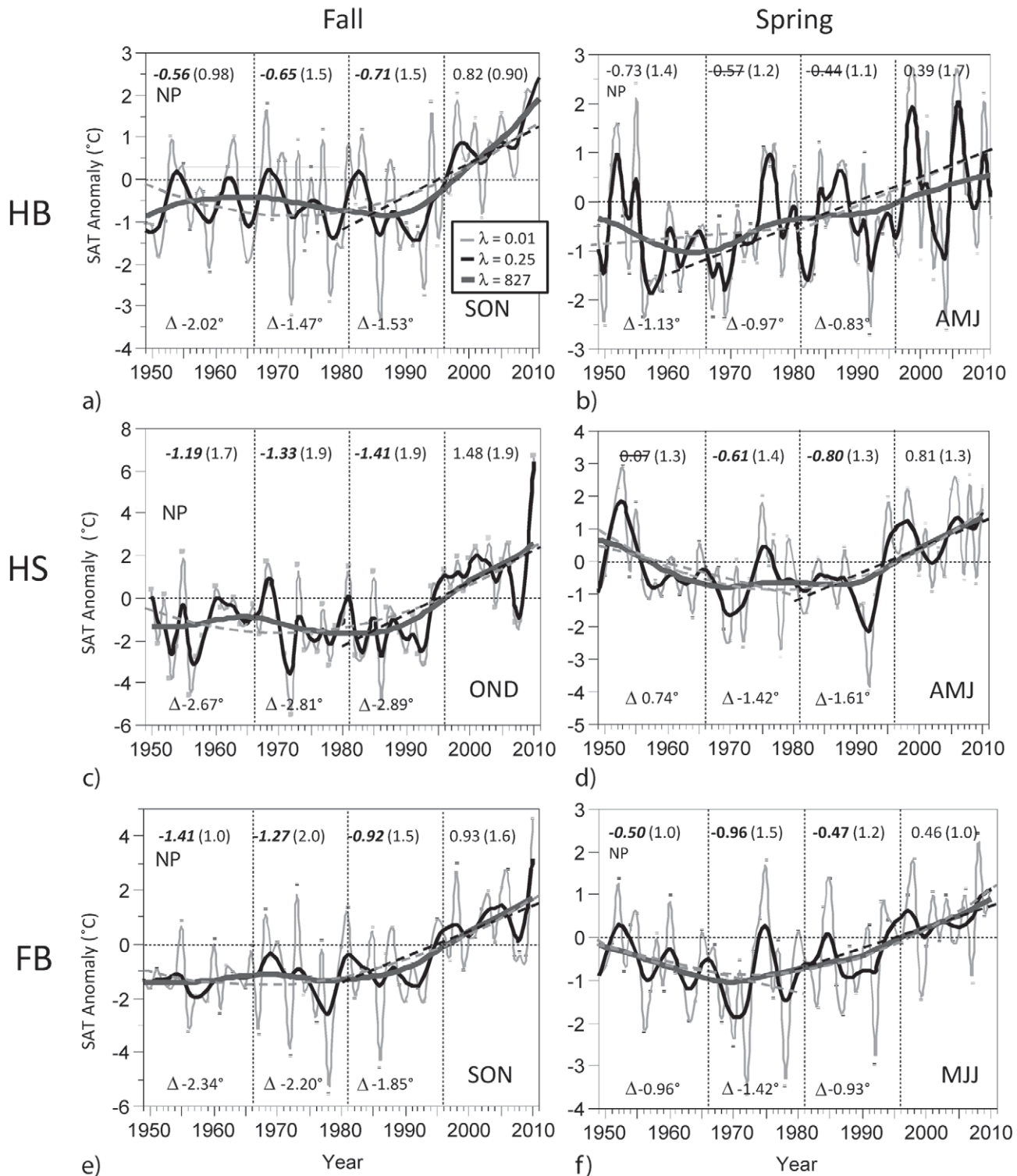
FIGURE 3. Fall and spring SAT anomalies surrounding Hudson Bay, Hudson Strait, and Foxe Basin. Seasons for each sub-region of the HBS are defined by the peak freeze-up/breakup, as defined by the three-month running mean, and are reflective of freeze and thaw sequences described in Hochheim and Barber (2010) and Hochheim et al. (2011). Spline fits (l) are used to highlight the interannual variation of SATs, their cyclical nature, and overall general trends. Second-order polynomial or linear fits (trends) are shown for years 1950–1979, 1980–2010, and 1950–2010 if significant at p = 0.05 or higher. Along the top of each graph are the mean temperature anomalies and standard deviations (in parentheses) for each 15-year interval. To denote if the 15-year mean SAT anomalies are significantly different from the 1996–2010 mean, mean SATs in bold italic are significantly different at p ≥ 0.01, in bold at p = 0.05, and in plain text at p = 0.1; NP = non parametric (p); strikethrough = not significant. Mean 15-year SAT differences (D) relative to 1996–2010 are located along the bottom of each graph.

KLAUS P. HOCHHEIM AND DAVID G. BARBER / 71

TABLE 2

Trends in fall SIE as a function of seasonal SATs.

Region	β (% SIE)	Std Error (%)	β (km²)	Std Error (km²)	r^2	p
HB	−14.42	1.3698	−133,730	±2594	0.79	<0.0001
HS	−15.01	1.4354	−28,420	±2718	0.80	<0.0001
FX	−14.41	1.4072	−27,288	±2665	0.79	<0.0001

SIE = sea ice extent, SATs = surface air temperatures.

For the Hudson Strait region, the three-week period of highest SIE variation occurs over WOYs 48–50 (26 November to 16 December). Mean SIE anomalies averaged over these weeks are highly correlated with Hudson Strait seasonal (OND) SATs (R^2 = 0.80, $p \leq 0.0001$) (Table 2). Two "outliers" were identified: 1986, an exceptionally cold year (−5.2 °C), and 2010, an exceptionally warm year (+6.7 °C). Both were outside the bounds required to create 100% SIE or 0% SIE during WOY 48–50. The mean SIE over 1980–2010 was 47% of the Hudson Strait area or 8.95×10^4 km². Every 1 °C increase in seasonal SAT resulted in a decrease in SIE by 15% (SE ±1.4%) of Hudson Strait area or 2.84×10^4 km² (±2.7 × 10³ km²). Seasonal SAT anomalies required to either generate an ice-free scenario or 100% SIE are +3.1 and −3.6 °C, respectively. The mean difference in SIE between the early and later part of the satellite record is 46% (±8.4%) or 8.71×10^4 km² (±1.59 × 10⁴ km²) (Fig. 4, part d). The decrease in SIE is associated with a 2.89 °C increase in mean SAT (Fig. 3, part c).

Foxe Basin freezes slightly earlier than the other regions within the HBS because of its more northerly latitude and the stronger continental influence from the surrounding landscape. The weeks of maximum variation of interannual SIE are best represented as the mean of WOY 44–46 (29 October–18 November), and the mean SIE for this period is highly correlated to SAT anomalies computed over SON (R^2 = 0.79, $p < 0.001$) (Fig. 4, part e, and Table 2). One outlier was identified (1986) that was beyond the SAT range required to generate 100% SIE.

The mean SIE for this period is 60.4% of the Foxe Basin area or 1.25×10^5 km². Every change in 1 °C results in a change in SIE of 14.4% (SE ±1.4%) (or 2.73×10^4 km² [±2.92 × 10³ km²]). The observed seasonal temperature range from 1980 to 2010 is approximately ±4.6 °C, and the mean estimated temperatures required to achieve 0 and 100% SIE over Foxe Basin is +4.3 and −2.7 °C for WOY 44–46. The mean difference in the SIE anomalies between the cooler and warmer regime is 29.2% (±8.0%) or 6.06×10^4 km² (±1.66 × 10⁴ km²) (Fig. 4, part f). The decrease in SIE coincides with a SAT increase of 1.85 °C.

Spring SIEs

Predicting spring SIEs requires consideration of not only spring SAT anomalies, but also fall (lag1) SATs and winds. Incorporating fall SATs in predicting spring SIE (and breakup date) is important as preconditioning of the ocean-atmosphere system has profound effects on late-season sea surface temperatures, the stability of the ocean mixed layer, and ultimately the timing of freeze-up and the thermodynamic and dynamic growth rates of ice extending into the winter period (e.g., Saucier and Dionne, 1998; Saucier et al., 2004; Joly et al., 2011). The approach taken here is consistent with

Hochheim et al. (2011), where both seasonal spring and fall (lag1) temperatures are considered, as well as dynamic forcing of late-season ice. Here we substitute late-season ice vorticity used in Hochheim et al. (2011) with U and V wind components.

Hudson Bay SIE computed over WOY 24–26 (11 June–1 July) is highly correlated (R^2 = 0.82) with seasonal three-month SAT anomalies ending June (AMJ), SATs from the previous fall ending November (SON lag1), and the U component wind anomaly from western Hudson Bay for (AMJ) (Table 3 and Fig. 5, part a). Nine temperature scenarios based the maximum seasonal temperature ranges observed (1980–2010) for the fall (±2.5 °C) and spring (±2.0 °C) stratified by three U wind anomaly scenarios, ±1.2 ms⁻¹ and normal (0) winds, were used to examine variations in SIEs (Fig. 5, part b). Based on the scenarios presented and associated regression parameters (Table 3), spring SAT anomalies alone provide the largest leverage on interannual SIE (±19% or 1.76×10^5 km²) (assuming normal fall SATs and winds), while fall temperatures had a leverage (±14.3% or 1.33×10^5 km²) (assuming normal spring SATs and winds). The maximum range of SIE anomalies based on both spring and fall temperatures (assuming normal winds) are approximately ±33.6% of Hudson Bay area (±3.11 × 10⁵ km²), while adding winds to the previous scenario increases the range of SIEs by ±10% to ±43.6% (or ±4.04 × 10⁵ km²). The combined effects of the three parameters are predictive of the potential interannual variation (range) of SIE in Hudson Bay.

The use of the U wind component in the above example was logical as it supports advection of ice offshore in western Hudson Bay and dynamic thickening of ice in central and southeastern Hudson Bay, a process that is modeled by Saucier et al. (2004) and others. The V wind component along the east coast of Hudson Bay was also examined as a regression variable based on modeling results in Wang et al. (1994). Wang et al. (1994) modeled ice velocity fields for the spring (mid-April) and summer (mid-July) and found that in the absence of wind forcing, a "large amount" of ice is exported out of northeastern Hudson Bay via local currents, especially during the April period when ocean current forcing is strong, versus mid-July when it is much weaker. Replacing the western Hudson Bay U wind component anomaly with V component wind anomalies (±1.0 ms⁻¹) of eastern Hudson Bay results in a higher coefficient of determination (R^2 = 0.88, $p \leq 0.0001$) (Table 3). The V component winds contribute about the same to SIE leverage of ±9.4% (or ±8.7 × 10⁴ km²) in Hudson Bay given normal spring and fall SATs. This suggests that very weak −V winds (northerlies) or +V winds may enhance early spring ice export in northeastern Hudson Bay as modeled by Wang et al. (1994). Fall SATs (±2.5 °C) alone provided mean leverage of ±15% (or ±1.4 × 10⁵ km²), while spring SATs (±2 °C) alone provided a potential leverage of ±32% (or ±2.97 × 10⁵ km²) on
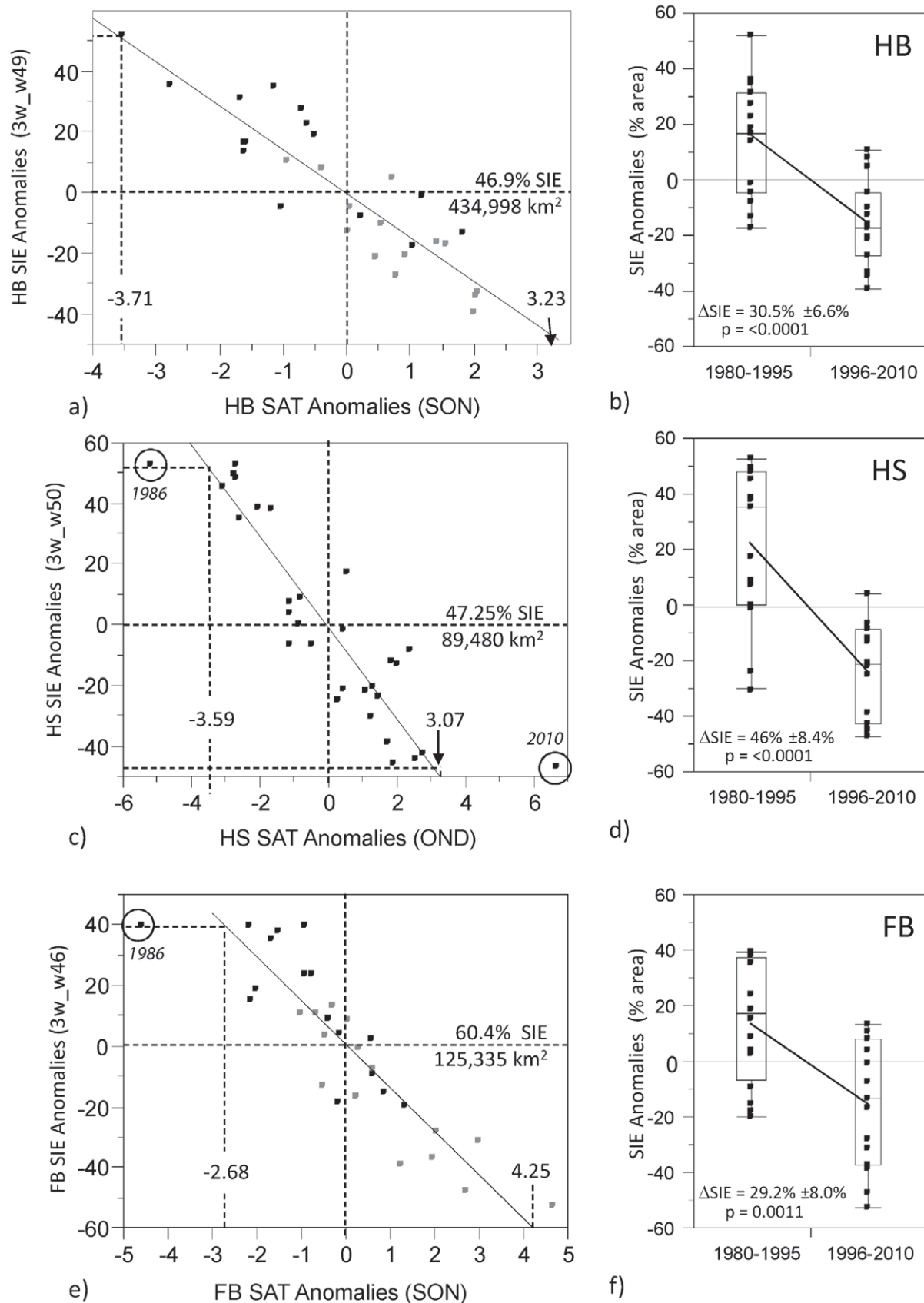
FIGURE 4. Regression relationships between SAT vs. sea ice extent (SIE) anomalies for (a) Hudson Bay, (c) Hudson Strait, and (e) Foxe Basin. Observations outside the 0–100% SIE predicted limits are considered outliers (circled). SAT anomalies required to meet 100% and 0% SIE are identified. Mean differences in SIEs (1980–1995 vs. 1996–2010) are shown for (b) Hudson Bay, (d) Hudson Strait, and (f) Foxe Basin. Significance tested using t-test assuming unequal variances.

KLAUS P. HOCHHEIM AND DAVID G. BARBER / 73

the observed interannual SIEs. The maximum observed range in predicted SIEs incorporating SATs and winds is ±41% (or ±3.8 × 10^5 km^2). As the melt season progresses, SAT anomalies become a more significant predictor ($R^2 = 87$, $p \leq 0.0001$) and winds become insignificant for both U and V components discussed (Table 3).

To put these model results in perspective, the general observed tendencies for both SAT and U winds in western Hudson Bay are shown in Figure 6, part a; note that spline fits are used in a qualitative sense to highlight the relative tendencies of SATs and wind over the observation period (1980–2010) and therefore mask the high interannual variations of the raw data used for statistical analysis. Note that both fall and spring SATs increase over time, as do the +U winds on the west coast and the +V winds on the

east coast. U winds have on average increased (+0.38 ms^{-1}) in the warmer period, as have the V winds in eastern Hudson Bay (+0.4 ms^{-1}). These shifts in winds are consistent with increased (+) ice vorticity within Hudson Bay relative to pre-1990s (Hochheim et al., 2011). The mean shift in the observed SIE was –23% (±5.8) of basin area ($p = 0.0007$) (Fig. 6, part b).

Hudson Strait SIE in early spring (4–24 June) is highly correlated ($R^2 = 0.78$) with spring (AMJ) and fall (OND lag1) SATs and spring (AMJ) U winds (Table 3 and Fig. 5, part c). The U winds are of particular interest in this case as the Hudson Strait has an east-west axis; negative U winds (easterlies) have the potential to retain ice in Hudson Strait and/or potentially promote ice import from the Labrador Sea. Positive U winds (westerlies) may enhance
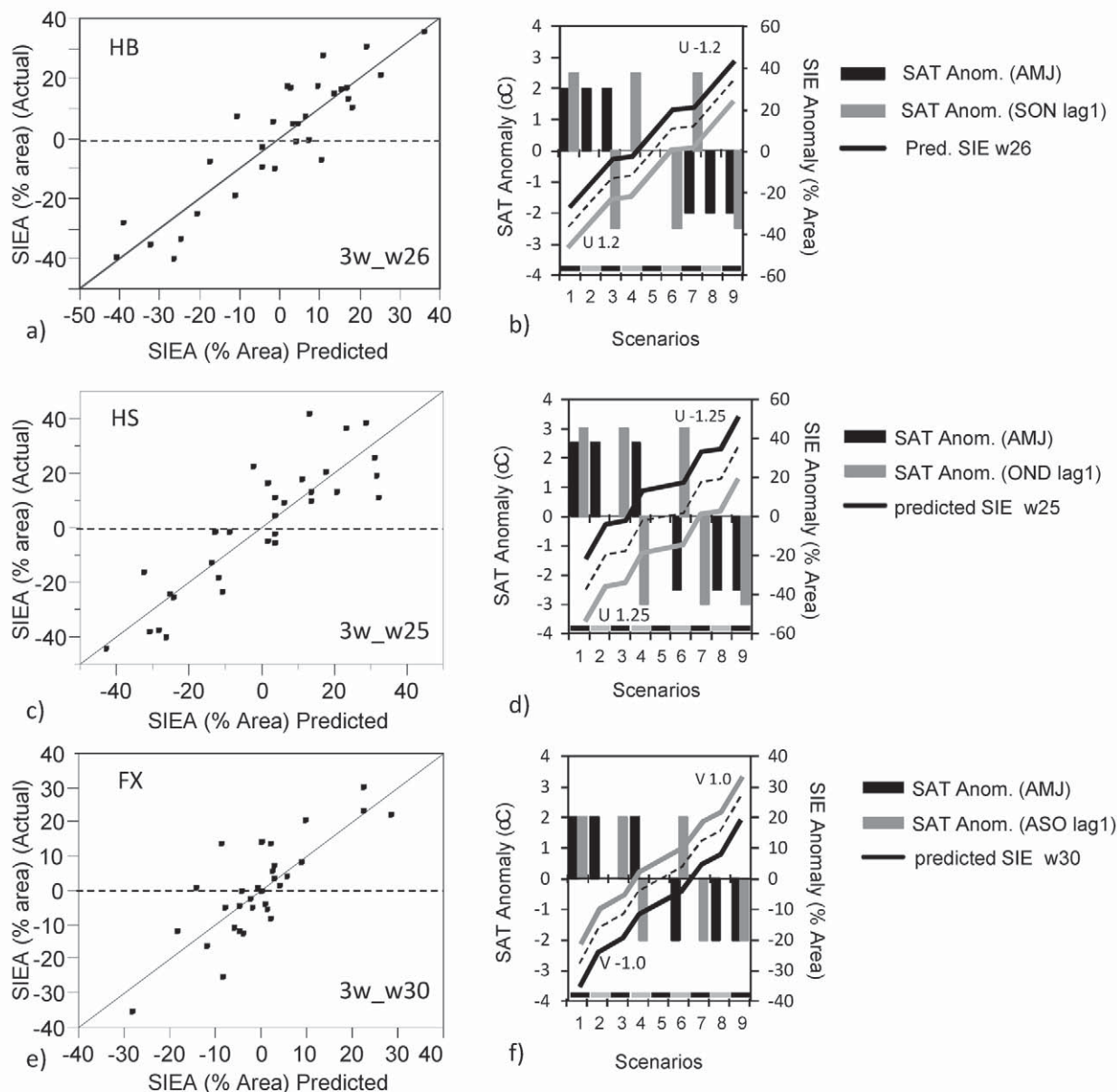
FIGURE 5. Predicted vs. observed SIEs for (a) Hudson Bay, (c) Hudson Strait, and (e) Foxe Basin. Model results show predicted changes in SIE as a function of spring and fall (lag1) SATs and winds (U or V) for (b) Hudson Bay, (d) Hudson Strait, and (f) Foxe Basin. Predicted SIEs are shown by three diagonal lines representing results stratified by the wind anomaly components (+ anomalies, normal [dotted line], and – anomalies).

TABLE 3

Regression coefficients used to predict changes in spring SIE for regions in the Hudson Bay System.

| Area	Regression Coef.	Estimate	Std. Error	Prob>(t)	R^2	RMSE
HB	Intercept	0.6401	1.5855	0.6893	0.82	8.80
W24-26	SAT anom. (AMJ)	–9.6527	1.1499	<0.0001		
	SAT anom. (SON lag1)	–5.7284	1.2228	<0.0001		
	HBW_U Wind (AMJ)	–8.3231	2.6302	0.0038		
HB	Intercept	–1.4594	1.3502	0.2879	0.88	7.35
W24-26	SAT anom. (AMJ)	–8.5080	0.9818	<0.0001		
	SAT anom. (SON lag1)	–6.0030	1.0212	<0.0001		
	HBE_V Wind (AMJ)	–9.3937	2.3937	0.0006		
HB	Intercept	–0.4532	1.2330	0.7160	0.87	6.84
W26-28	SAT anom. (MJJ)	–14.6640	1.2735	<0.0001		
	SAT anom. (SON lag1)	–4.0396	0.9164	0.0004		
HS	Intercept	–1.3995	2.1519	0.5210	0.78	11.80
W23-25	SAT anom. (AMJ)	–7.7635	1.5604	<0.0001		
	SAT anom. (OND lag1)	–5.3949	1.1785	<0.0001		
	U Winds anom. (AMJ)	–12.4020	2.9688	<0.0001		
FX	Intercept	–0.8001	1.5975	0.6205	0.65	8.83
W28-30	SAT anom. (MJJ)	–7.9485	1.4653	<0.0001		
	SAT anom. (ASO lag1)	–5.9641	1.3754	0.0002		
	V Winds (AMJ)	7.3943	2.5751	0.0079		

export of ice out of Hudson Strait or alternatively inhibit ice import from the Labrador Sea.

What is different relative to the Hudson Bay result is the larger potential leverage of winds on SIE given a more direct outlet to the Labrador Sea. The U wind forcing component by itself has the potential effect of varying interannual SIE by ±15.7% (or ±2.97 × 10⁴ km²) based on parameters used in Figure 5, part d, and Table 3. Based on the model results (assuming normal winds and normal fall temperatures), Hudson Strait spring SAT anomalies (±2.5 °C) are predictive of ±18.8% (or ±3.55 × 10⁴ km²) change in interannual SIE (WOY 23–25). Assuming normal U winds and spring SATs, fall (OND lag1) temperature anomalies (±3 °C) have a mean SIE leverage of ±17.1% of Hudson Strait area (or 3.2 × 10⁴ km²). Considering the joint effect of fall (lag1) and spring SATs (assuming normal U winds), SIE in Hudson Strait is predicted to vary by ±36% of Hudson Strait area (or ±6.8 × 10⁴ km²). The potential predicted range of SIEs given all three factors has the potential of creating an ice-free scenario to one with 100% SIE. The Hudson Strait example is interesting in that both fall (lag1) and spring SAT anomalies can potentially have similar leverage on SIE given the right scenario, suggesting that preconditioning of the ice in fall can play a significant role in spring breakup.

To put results in context, part c in Figure 6 shows spline fits for the observed data on SATs and U winds over Hudson Strait. Both fall and spring temperature anomalies tended to be more negative prior to 1995, after which they became predominantly positive (Section 3.1). The U wind anomalies, though variable throughout the 1980–2010 period, increased slightly (+0.3 ms⁻¹) during the later period. In Figure 7, parts a and b show the wind

vectors and associated atmospheric pressure patterns over Hudson Strait for select years where the U winds were either strongly positive or negative in the spring (AMJ). An increase in positive U winds would support a reduction of SIE through dynamic forcing (potential export). The mean differences in SIE between the cooler and warmer periods are –33% ± 6.2% (or 6.25 × 10⁴ km² ±1.2 × 10⁴ km²) (Fig. 6, part d). The mean difference in SIE corresponds to a mean temperature increase of 1.6 °C in the spring and mean increase of 2.89 °C in the fall (Fig. 3, parts c and d).

The early season Foxe Basin spring SIE (WOY 28–30) was best correlated to seasonal spring SATs (MJJ) together with the previous fall's (ASO lag1) SATs and V winds (AMJ) over the southern half of the Foxe Basin (R^2 = 0.65); the lower R^2 was due to an anomalous value in V winds, which was retained due to the low *n;* R^2 improves to 0.74 with the outlier removed. The model results using the approximate upper and lower limits of the data are presented in Figure 5, part e, and Table 3. The meridional (V) wind component was used for its potential to move ice southward out of the Foxe Basin. Based on the parameters in Figure 5, part f, SIE anomalies can vary ±7.4% (percent area of the Foxe Basin), or 1.5 × 10⁴ km² based on the V winds alone. Assuming normal spring SATs and V winds (0), fall temperatures can account for up to ±12% of the interannual SIE variation (or ±2.5 × 10⁴ km²) during the spring period. Spring SATs alone provide a leverage of up to ±20% (±4.12 × 10⁴ km²). Combining the potential impact of both fall and spring SATs (±2.0 °C) (assuming normal winds), SIEs can vary ±35% of basin or 7.22 × 10⁴ km². Add the potential effect of V winds on SATs, and SIE could vary by as much as ±46% or ±9.55 × 10⁴ km² given the model constrains for WOY 28–30.

KLAUS P. HOCHHEIM AND DAVID G. BARBER / 75
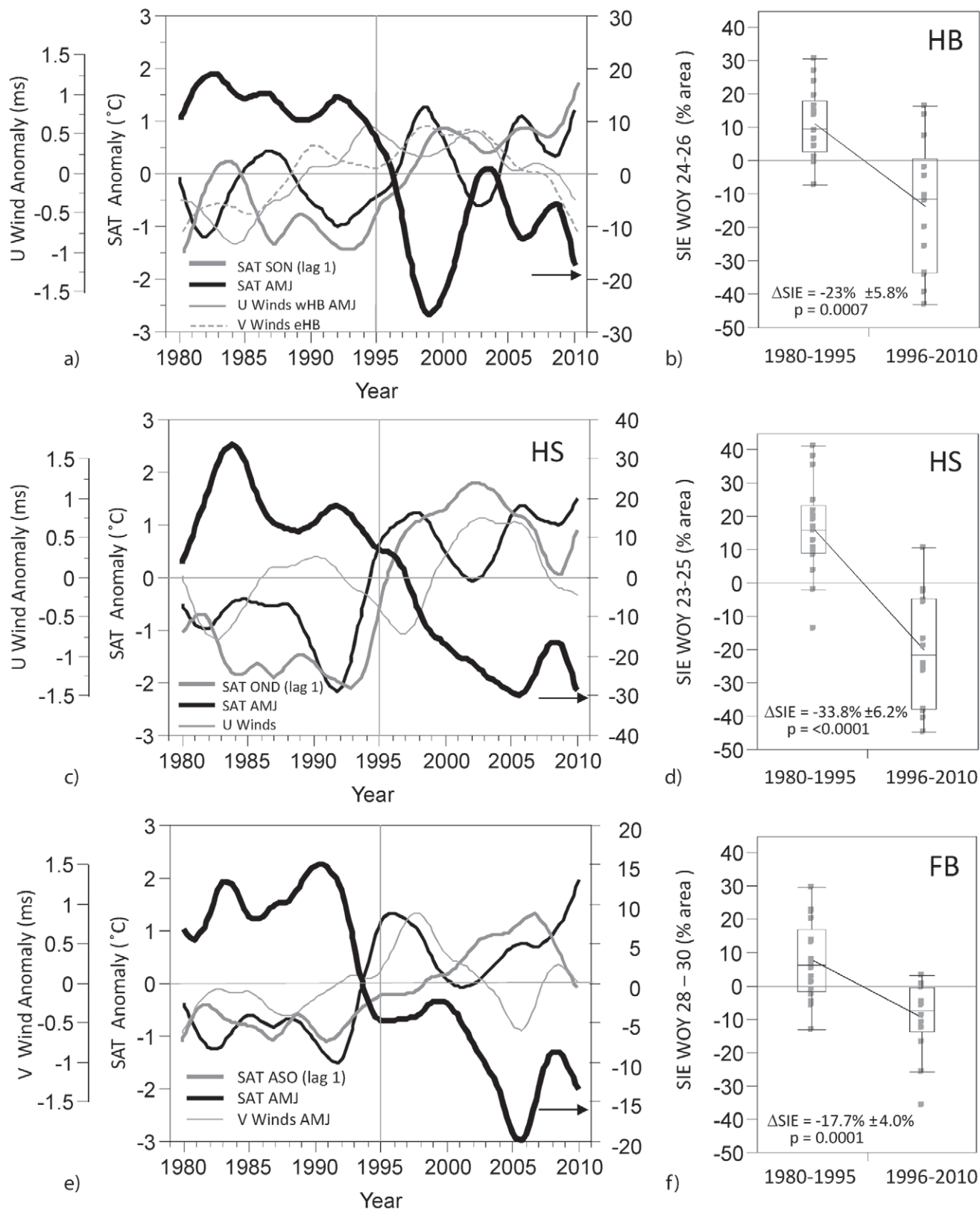
FIGURE 6. (a, c, e) Graphs showing the general tendencies of spring SIE (black bold line) as a function of spring and fall (lag1) SATs and winds per region using spline fits (l = 2.25). (b, d, f) The distribution of SIEs during the cooler (1980–1995) and warmer (1996–2010) climate regime and the resulting mean change in SIE. Significance based on t-test assuming unequal variances.

TABLE 4

Regression parameters for SAT anomaly vs. freeze-up date (50% base on sea ice concentrations (SICs) ≥ 60%).

Area	Regression Coef.	Estimate	Std. Error	Prob.	R^2	RMSE
HB	Intercept	0.0042	0.1158		0.72	0.64
	SAT anom. (SON)	0.7135	0.0821	<0.0001		
HS	Intercept	–0.0046	0.1359		0.81	0.76
	SAT anom. (OND)	0.6655	0.0562	<0.0001		
FX	Intercept	0.0006	0.1369		0.81	0.76
	SAT anom. (SON)	0.8786	0.0781	<0.0001		

Figure 6, part e, shows the general tendencies for fall (lag1) and spring SATs and V winds over 1980–2010 and their effect on SIE. The mean difference in SIE between the cooler and warmer climate regimes (Fig. 6, part f) is –17.7% (or 3.67×10^4 km²; p = 0.0001). Wind vectors over Foxe Basin representing select years of strongly negative and positive V winds are illustrated in Figure 7, parts c and d. Strong negative (positive) V winds are associated with a low (high) pressure over Greenland/Baffin Bay.

CHANGES IN FREEZE-UP AND BREAKUP DATES

The previous data show trends in three-week mean SIEs in relation to seasonal SATs and winds during a fixed period of maximum interannual variation. The following results are based on weekly data where freeze-up and breakup dates are defined as 50% cover of SICs ≥60%.

Freeze-up Dates

The range of freeze-up dates for Hudson Bay (1980–2010) is five weeks (–2.77 to 2.23), corresponding to a range of seasonal SAT (SON) of –3.5 to 2.1 °C (Fig. 8, part a). Seasonal SATs are moderately related to freeze-up anomaly (R^2 = 0.72; p ≤ 0.0001); the regression relationship predicts that a 1 °C increase in seasonal SAT delays freeze-up date by 0.71 weeks (Table 4). Based on the observed data, freeze-up dates from 1980 to 1995 were on average 0.77 weeks earlier than normal, whereas freeze-up dates in the warmer regime (1996–2010) were on average 0.83 weeks later resulting in a mean difference of 1.6 (±0.32) weeks (p ≤ 0.0001) between the two periods; the median difference in freeze-up date was marginally larger at 2.0 weeks.

The range of freeze-up anomaly dates in Hudson Strait over 1980–2010 was 8 weeks (–3.65 to 4.35 weeks), corresponding to a range of seasonal SATs (OND) anomalies of –5.2 to 6.7 °C, the bulk of the temperatures are with ±3 °C range (Fig. 8, part c). Regional surface air temperatures surrounding Hudson Strait were highly correlated with week of freeze-up (R^2 = 0.81, p ≤ 0.0001). The regression result suggests that every 1 °C increase in seasonal SAT freeze-up date is delayed by 0.67 weeks. The mean of freeze-up date anomalies from 1980 to 1995 is –1.15 weeks (weeks earlier) compared to 1996–2010 where the mean freeze-up date is 1.22 weeks later, resulting in a mean difference of 2.4 (±0.45) weeks (p ≤ 0.001), which coincides to a mean SAT increase of 2.9 °C. The difference in median freeze-up dates for the two periods (–1.65 vs. 1.35 weeks) is about 3.0 weeks between the two periods.

Foxe Basin freeze-up anomalies range from –5.7 to 6.7 weeks corresponding to a regional SAT range of ±4.6 °C, the majority of the SATs from 1980–2010 range between –2 to 3 °C. The freeze-up dates are highly correlated with interannual SATs (R^2 = 0.81, RMSE = 0.76, p ≤ 0.0001), predicting that with every 1 °C increase in SAT, freeze-up is delayed by 0.88 weeks. The mean freeze-up dates between the cooler and warmer periods are –0.98 vs. +1.0 week, resulting in a mean delay of 2.0 (±0.51) weeks in freeze-up (Fig. 8, part f). The median response to freeze-up date for the two periods is –1.29 vs. 0.71, respectively, thus matching the mean response. The mean two-week delay in freeze-up corresponds to a mean temperature increase of 1.9 °C.

Breakup Dates

Breakup dates are examined based on regional fall (lag1) and spring SAT and winds, as were SIEs. Based on the regression coefficients presented in Table 5 and the input parameters representative for each basin (Fig. 9, parts a, c, and e), the relative leverage of SATs and winds are examined in relation to sea ice breakup date.

For the Hudson Bay area, regional spring and fall (lag1) SATs and U winds were highly predictive of breakup date (R^2 = 0.83) (Table 5). The maximum observed range in breakup dates for Hudson Bay (1980–2010) is 2.74 to –2.26, or 5 weeks. Spring (MJJ) SAT anomalies alone (±2.0 °C) (assuming normal winds and fall SATs) account for most of the observed variation in breakup date, providing a leverage of ±1.9 weeks. Fall SATs (±2.5 °C) provide a leverage of ±0.93 weeks assuming normal spring SAT and winds; the U component of winds (AMJ) alone provides very limited leverage (±0.44 weeks), assuming the parameter limits used in Figure 9, part a. The maximum range of melt-out dates using both spring and fall SAT provided a range of ±2.9 weeks, the maximum observed range of breakup date combining the contribution of SATs and winds was estimated at ±3.3 weeks. The observed mean breakup anomalies for the cooler and warmer period result in a mean difference in breakup date of –1.53 weeks (±0.39) (p = 0.0002) (Fig. 9, part b).

As for SIE in Section 3.3, another trial was run for Hudson Bay using (AMJ) SATs (±2.5 °C) and the same fall (lag1) temperature range (±2.5 °C) and substituting west coast U winds with east coast V winds. The potential leverage of V wind alone on breakup date increases to ±0.7 weeks from 0.44 (note, winds tend to have more leverage using earlier spring SATs). The leverage of fall SATs (lag1) on breakup date also increases to ±0.93 assuming normal spring (AMJ) and V winds. Spring SATs alone have a
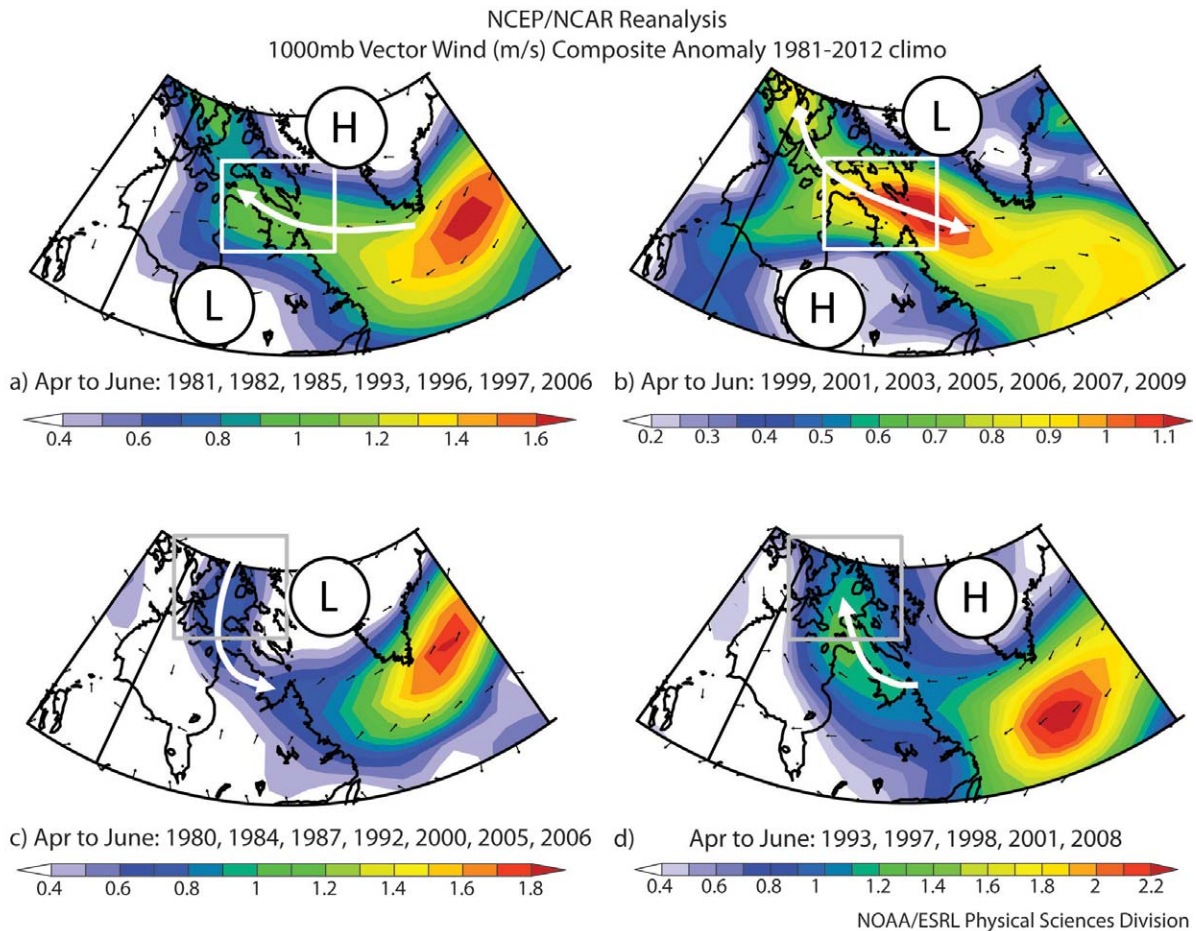
FIGURE 7. Dominant surface wind vectors in the spring (AMJ) representing (a) years with strong negative U winds over Hudson Strait, and (b) years with strong positive U winds over Hudson Strait. Spring (AMJ) wind vectors over Foxe Basin representing years with (c) strong negative V wind anomalies and (d) with strong positive V wind anomalies. Associated atmospheric pressure anomalies are shown.

TABLE 5

Regression coefficients used to predict spring break-up anomalies.

Area	Regression Coef.	Estimate	Std. Error	Prob	R^2	RMSE
HB	Intercept	−0.0433	0.1035	0.6785	0.83	0.57
	SAT anom. MJJ	−0.9703	0.1068	<0.0001		
	SAT anom. SON lag 1	−0.3705	0.0791	<0.0001		
	HBW_U Wind (AMJ)	−0.3645	0.1694	0.0406		
HB	Intercept	−0.1058	0.1102	0.3457	0.82	0.59
	SAT anom. AMJ	−0.5350	0.0801	<0.0001		
	SAT anom. SON lag 1	−0.3888	0.0834	<0.0001		
	HBE_V Wind AMJ	−0.6951	0.1952	0.0015		
HS	Intercept	−0.1346	0.1951	0.4950	0.72	0.69
	SAT anom. MJJ	−0.7372	0.1779	0.0003		
	SAT anom. OND lag 1	−0.5132	0.1047	<0.0001		
	U Winds AMJ an	−0.8113	0.2718	0.0060		
FX	Intercept	−0.0666	0.1502	0.0167	0.67	0.83
	SAT anom. MJJ	−0.8177	0.1378	<0.0001		
	SAT anom. ASO lag 1	−0.5070	0.1293	0.0005		
	V Winds AMJ	0.9064	0.2421	0.0009		
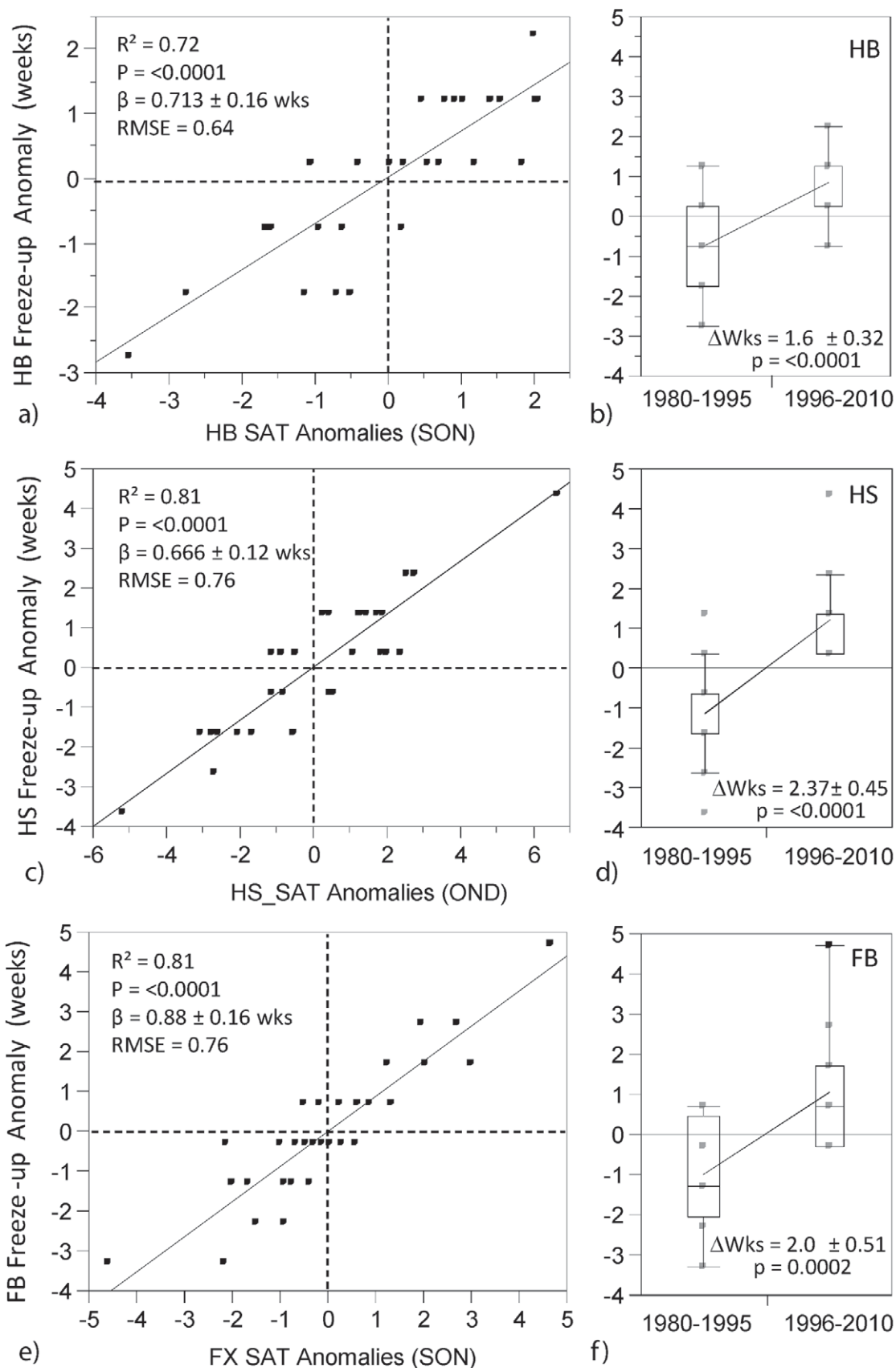
FIGURE 8. Observed vs. predicted freeze-up dates based on fall SATs for (a) Hudson Bay, (c) Hudson Strait, and (e) Foxe Basin. (b, d, f) The distribution of freeze-up dates during the cooler (1980–1995) and warmer (1996–2010) climate regime and the resulting mean change in freeze-up date (weeks). Significance of differences based on t-test assuming unequal variances.

KLAUS P. HOCHHEIM AND DAVID G. BARBER / 79

leverage of ±1.34 weeks, while the potential leverage of both spring and fall (lag1) SATs increases to a range of ±2.3 weeks. Combining SATs and V winds, the potential interannual variation in mean breakup date increases to ±3.0 weeks. It's interesting that fall (lag1) and +V winds (assuming normal spring SATs) have a similar (marginally higher) potential leverage than spring SATs alone (±1.6 vs. ±1.3 weeks).

Regional SATs and winds are predictive ($R^2 = 0.72$) (Table 5) of breakup dates in Hudson Strait. Based on the observed data (1980–2010), the range in breakup dates in the Hudson Strait is ±3.5 weeks; these are a result of fall (SON, lag 1) SATs ranging from –5.2 to +2.8 °C and spring (MJJ) SATs ranging from –3.1 to 2.7 °C (1980–2010); most seasonal fall SATs ranged between ±3 °C vs. ±2.5 °C in spring. Assuming normal SATs for both the fall (lag1) and spring, the U winds provide a leverage of ±1.0 week, with +U winds (westerly) associated with earlier melt-out dates (potential ice export) versus –U winds, which may act to retain ice within Hudson Strait. Assuming normal winds and fall (lag 1) temperatures, spring SATs provide a leverage of ±1.6 weeks; fall temperatures alone provide a leverage of ±1.3 weeks based on parameters used in Figure 9, part c. The combined leverage of both fall (lag1) and spring SAT is potentially ±3.1 weeks on breakup date. The maximum predicted range in breakup dates based on both seasonal SATs and winds is approximately ±4.2 weeks; the actual observed range in breakup dates in Hudson Strait from 1980 to 2012 was lower (±3.5 weeks). The mean difference in breakup date between the cooler and warmer climate regime is 2.5 (±0.53) weeks ($p \leq 0.0001$) (Fig. 9, part d). The difference in median breakup dates was three weeks.

In Foxe Basin, breakup date is moderately correlated ($R^2 = 0.67$) (Table 5) with SATs and winds. The maximum observed range in breakup date is 7 weeks (1980 to 2010), but they typically vary ±2.5 weeks. Similar to Hudson Strait, the wind component plays a significant role in defining breakup date in Foxe Basin. The leverage of V wind component on breakup is estimated at ±0.91 weeks assuming normal fall (lag1) and spring temperatures (Figure 9e), similar to Hudson Strait. The leverage of fall (ASO, lag1) SATs (±2˚C) alone is up to ±1.0 weeks; the mean leverage of spring (MJJ) SATs alone is ±1.6 weeks. Based on the SAT and V wind limits used, the maximum predicted variation in breakup date is ±3.6 weeks, a range of 7.2 weeks, closely approximating the observed range (+2.8 to –4.2 weeks). The mean difference between ice breakup between the first half of the satellite record and the second half is 1.5 (±0.4) weeks ($p = 0.0015$) (Fig. 9, part f); the difference in median breakup dates between the two periods is 1.0 week.

Cumulative Changes in Sea Ice

The cumulative effects of shifts toward later freeze-up and earlier breakup culminate in a longer open water (OW) season (Table 6). The mean shifts toward a longer open water season (1980–1995 vs. 1996–2010) is ~3 weeks for Hudson Bay, almost 5 weeks on average for Hudson Strait, and 3.5 weeks for Foxe Basin (Table 6). Noteworthy also is the range of the open water season in weeks around the normal over 1980–2010, which is ±4.5 weeks for Hudson Bay and about ±6 weeks for Hudson Strait and Foxe Basin. Differences in the observed and predicted mean ΔOW are attributable to factors such as water temperature and salinity, ocean circulation, and riverine influence at subregional scales.

The spatial distribution of shifts in median freeze-up date and breakup date and the resulting cumulative change are shown in Figure 10, parts a–c. The greatest median shifts during freeze-up occur in the eastern portion of Hudson Bay, Southern Foxe Basin, and within Hudson Strait, with shifts ranging from 2 to 3 weeks (Fig. 8, part a). During breakup, some of the largest changes in Hudson Bay are observed along the northwestern coast (2–5 weeks) and southwestern coast (2–3 weeks); large changes also occur along much of the eastern coast, particularly in the northeast (2–5 weeks). The central portion of Hudson Bay shows little change in median breakup date as ice is generally advected to this location because of winds and currents. In Hochheim et al. (2011), both the Canadian Ice Service data and passive microwave data showed minimal trends in sea ice concentration anomalies (including some positive trends, though nonsignificant) west of the Belcher Islands. In Foxe Basin the median shift in the fall is only 1 week, although the Foxe Channel area has a median shift of 2 weeks during breakup. Hudson Strait has the largest shifts in median breakup dates (2–5 weeks).

Cumulative median shifts in Hudson Bay are generally on the order of 3–4 weeks, with the largest shifts and the northwest and eastern coast 3–6 weeks. The largest changes in Foxe Basin occur in Foxe Channel (4–5 weeks) and more generally 2–3 weeks. In Hudson Strait the median shift has been 6 weeks.

Conclusions

The changes documented above relate to a broader signal of changes occurring in the Arctic. However, the changes in the HBS appear to be occurring more rapidly and are more strongly correlated to atmospheric forcing relative to other arctic regions, such as the Beaufort Sea and the Canadian Arctic Archipelago, where ice climatology is significantly more complex due to the interplay of different ice ages, among other factors (Deser and Teng, 2008).

TABLE 6

Mean shifts in dates (weeks) for freeze-up and break-up relative to the normal when comparing 1980–1995 with 1996–2010; the observed change in open water season (Mean DOW), and predicted change in open water season (Predicted Mean DOW); followed by cumulative shift expressed as an increase in the maximum range of open water season relative to the normal over 1980–2010.

| Region	Δ Freeze-up (wks)*	Δ Break-up (wks)**	Mean ΔOW	Predicted Mean ΔOW	Range OW (wks)
HB	1.6 (± 0.32)	1.53 (± 0.39)	3.13 (± 0.57)	2.05 (±0.38)	–4.5 to 4.5
HS	2.37 (± 0.45)	2.48 (± 0.53)	4.85 (± 0.76)	3.32 (±0.96)	–6.1 to 5.9
FX	2 (± 0.51)	1.48 (± 0.42)	3.50 (± 0.85)	2.1 (±0.48)	–5.1 to 6.9

*Weeks later; **weeks earlier.
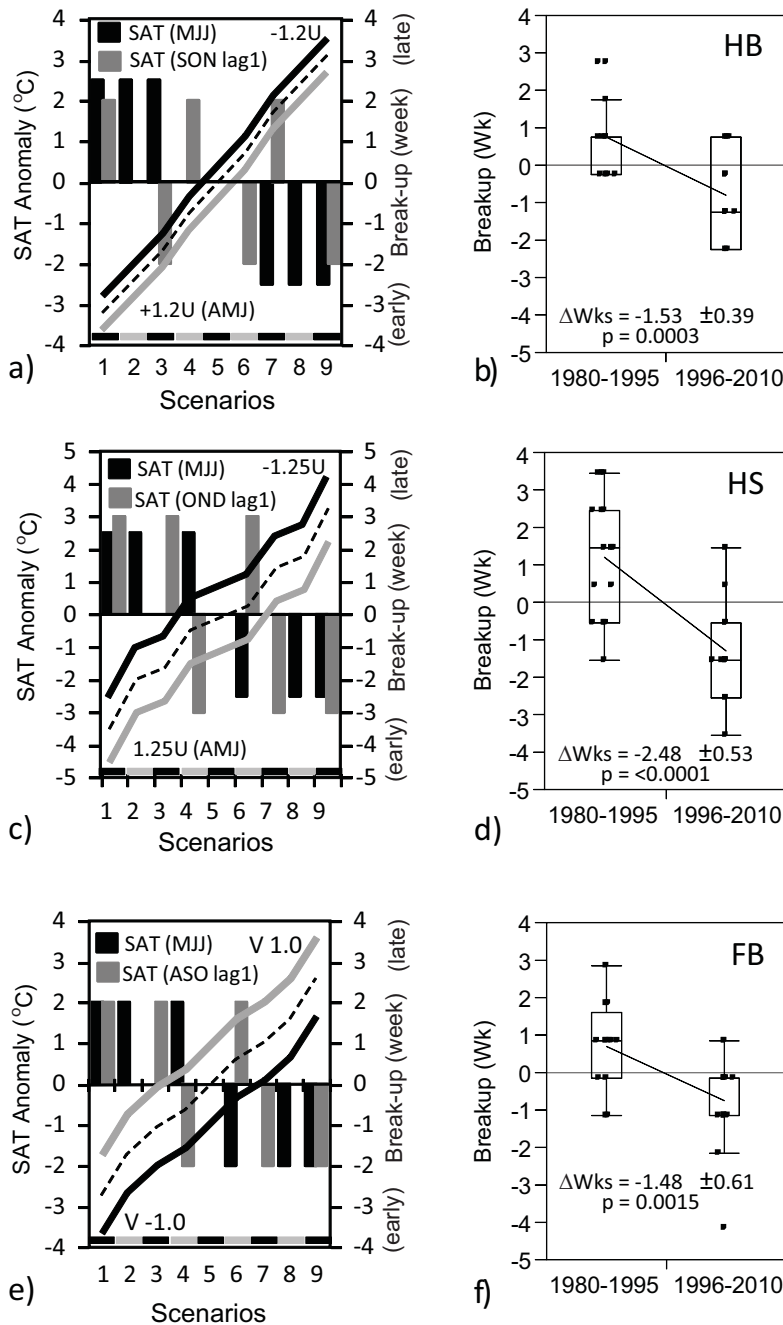
FIGURE 9. Predicted breakup dates based on spring and fall (lag1) SATs stratified by the wind component (± U or V winds), for (a) Hudson Bay, (c) Hudson Strait, and (e) Foxe Basin. (b, d, f) The distribution of observed breakup dates during the cooler (1980–1995) and warmer (1996–2010) climate regime and the resulting mean change in breakup date (weeks). Significance of difference based on t-test assuming unequal variances.

Surface air temperatures (SATs) have increased universally over the HBS when comparing the early portion of the satellite record (1980–1995) to the later (1996–2010) for both the fall and spring period. SAT increases were relatively higher in the fall (1.53–2.89 °C) versus the spring (0.83–1.61 °C). The relatively higher SATs in fall are in agreement with SATs used by Joly et al. (2011) in an atmospheric forcing response study. The spatial distribution of SAT trends were highest over Hudson Strait and Foxe Basin; the largest trends surrounding Hudson Bay were located along the eastern and northwestern coast. Interannual variations in surface air temperature remain high despite the recent shift to warmer regional temperatures.

SIE in the fall is highly correlated with three-month mean seasonal SATs (R^2 = 0.79–0.82) across all basins, the mean response to a 1 °C increase in SAT is a decrease of SIE on the order of 14.4–15.0% (of basin area). In the spring, SIE extent is best measured incorporating fall (lag1) and spring SATs and winds. In the breakup period, both spring and fall SATs combined proportionately account for most of the interannual variation in SIE for Hudson Bay and Hudson Strait (77% and 70%, respectively), and 81% in Foxe Basin, with the remaining leverage for explained variability accounted for by wind forcing. Wind forcing contribution of observed SIE is highest in Hudson Strait, followed by Hudson Bay. Based on the model results, fall (lag 1) temperatures proportionately contribute 30 to 36% of the total observed variation of SIE, thus highlighting the significance of environmental conditions in the fall and their potential impact of ice growth into the winter season (preconditioning).

KLAUS P. HOCHHEIM AND DAVID G. BARBER / 81
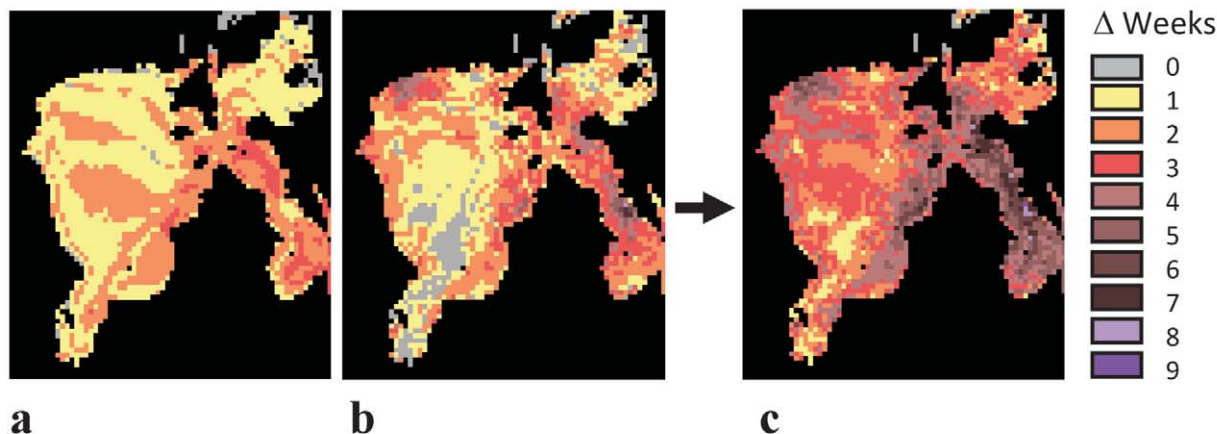
FIGURE 10. The spatial distribution of changes (D) in (a) median freeze-up date (1980–1995 vs. 1996–2010), weeks later; (b) median breakup date (1980–1995 vs. 1996–2010), weeks earlier; and (c) cumulative change in weeks indicating a longer open water season.

Freeze-up dates are all closely related to seasonal fall SATs. For every 1 °C increase in SAT, freeze-up is delayed by approximately 0.7 weeks for Hudson Bay and Hudson Strait and 0.9 weeks in Foxe Basin. With a general increase in SATs throughout the HBS, freeze-up date has been delayed 1.6 to 2.4 weeks on average (Hudson Bay and Hudson Strait, respectively). Breakup in the spring is on average 1.5 weeks earlier for Hudson Bay and Foxe Basin (1980–1995 vs. 1996–2010) and 2.5 weeks earlier in Hudson Strait. Taking into account variations in fall (lag1) and spring temperatures and winds, the regression models suggest that both fall and spring SATs combined proportionately account for about 75% of the explained interannual variation in the observed breakup dates across all basins, while wind forcing accounts for the remaining 25%. The contribution of fall (lag1) SATs to breakup date vary between 28% and 33% of the total explained variation depending on the region. The combined effect of later freeze-up dates and earlier breakup dates is that, since 1996, the open water season has on average increased by 3.1 (±0.6) weeks in Hudson Bay, 4.9 (±0.8) weeks in Hudson Strait, and 3.5 (±0.9) weeks in Foxe Basin.

Acknowledgments

References Cited

Comiso, J. C., 2000 [updated 2011]: Bootstrap Sea Ice Concentrations from Nimbus-7 SMMR and DMSP SSM/I-SSMIS. Version 2. (1980–2010). Boulder, Colorado, U.S.A.: NASA DAAC at the National Snow and Ice Data Center.

Déry, S. J., and Wood, E. F., 2004: Teleconnection between the Arctic Oscillation and Hudson Bay river discharge, *Geophysical Research Letters*, 31: L18205, doi: http://dx.doi.org/10.1029/2004GL020729.

Déry, S. J., Stieglitz, M., McKenna, E. C., and Wood, E. F., 2005: Characteristics and trends of river discharge into Hudson, James, and Ungava Bays, 1964–2000. *Journal of Climate*, 18: 2540–2557.

Deser, C., and Teng, H., 2008: Evolution of Arctic sea ice concentration trends and the role of atmospheric circulation forcing, 1979–2007. *Geophysical Research Letters*, 35: L02504, doi: http://dx.doi.org/10.1029/2007GL032023.

Environment Canada, 2013: About Climate Trends and Variations Bulletin (CTVB), <http://www.ec.gc.ca/adsc-cmda/default.asp?lang=En&n=D48C5C94-1>.

Etkin, D. A., 1991: Break-up in Hudson Bay: its sensitivity to air temperatures and implications for climate warming. *Climatological Bulletin*, 25: 21–34.

Gagnon, A. S., and Gough, W. A., 2005: Trends in the dates of ice freeze-up and breakup over Hudson Bay, Canada. *Arctic*, 58: 370–382.

Galbraith, P. S., and Larouche, P., 2011: Sea-surface temperature in Hudson Bay and Hudson Strait in relation to air temperature and ice cover breakup, 1985–2009. *Journal of Marine Systems,* 87: 66–78, doi: http://dx.doi.org/10.1016/j.jmarsys.2011.03.002.

Hochheim, K. P., and Barber, D. G., 2010: Atmospheric forcing of sea ice in Hudson Bay during the fall period, 1980–2005. *Journal of Geophysical Research*, 115: C05009, doi: http://dx.doi.org/10.1029/2009JC005334.

Hochheim, K. P., Lukovich, J. V., and Barber, D. G., 2011: Atmospheric forcing of sea ice in Hudson Bay during the spring period, 1980–2005. *Journal of Marine Systems*, 88: 476–487, doi: http://dx.doi.org/10.1016/j.jmarsys.2011.05.003

Hurrell, J. W., Hoerling, M. P., Phillips, A. S., Xu, T., 2004: Twentieth century North Atlantic climate change. Part I: assessing determinism. *Climate Dynamics*, 23: 371–389.

Hurrell, J. W., Visbeck, M., Busalacchi, A., Clarke, R. A., Delworth, T. L., Dickson, R. R., Johns, W. E., Koltermann, K. P., Kushnir, Y., Marshall, D., Mauritzen, C., McCartney, M. S., Piola, A., Reason, C., Reverdin, G., Schott, F., Sutton. R., Wainer, I., and Wright, D., 2006: Atlantic climate variability and predictability: a CLIVAR perspective. *Journal of Climate*, 19: 5100–5121.

Joly, S., Senneville, S., Caya, D., Saucier, F. J., 2011: Sensitivity of Hudson Bay sea ice and ocean climate to atmospheric temperature

forcing. *Climate Dynamics*, 36: 1835–1849, doi: http://dx.doi.org/10.1007/s00382-009-0731-4.

Kinnard, C., Zdanowicz, C. M., Fisher, D. A., Alt, B., and McCourt, S., 2006: Climatic analysis of sea-ice variability in the Canadian Arctic from operational charts, 1980–2004. *Annals of Glaciology*, 44: 391–402, doi: http://dx.doi.org/10.3189/172756406781811123.

Mysak, L. A., Ingram, R. G., Wang, J., Van der Baaren, A., 1996: The anomalous sea-ice extent in Hudson Bay, Baffin Bay and the Labrador Sea during three simultaneous NAO and ENSO episodes. *Atmosphere-Ocean*, 34: 313–343.

NOAA Earth System Research Laboratory, 2011: NCEP_Reanalysis 2 data. Boulder, Colorado, U.S.A.: NOAA/OAR/ESRL PSD, <http://www.esrl.noaa.gov/psd/>.

Parkinson, C. L., and Cavalieri, D. J., 1989: Arctic sea ice 1973–1987: seasonal, regional, and interannual variability. *Journal of Geophysical Research*, 94: 14499–14523.

Prinsenberg, S. J., 1986a: The circulation pattern and current structure of Hudson Bay. *In* Martini, E. P. (ed.), *Canadian Inland Seas*. Oceanography Series 44. New York: Elsevier, 187–203.

Prinsenberg, S. J., 1986b: On the physical oceanography of Foxe Basin. *In* Martini, E. P. (ed.), *Canadian Inland Seas*, Oceanography Series 44. New York: Elsevier, 217–236.

Prinsenberg, S. J., Peterson, I. K., Narayanan, S., and Umoh, J. U., 1997: Interaction between atmosphere, ice cover, and ocean off Labrador and Newfoundland from 1962 to 1992. *Canadian Journal of Fisheries and Aquatic Sciences*, 54: 30–39, doi: http://dx.doi.org/10.1139/cjfas-54-S1-30.

Qian, M., Jones, C., Laprise, R., Caya, D., 2008: The influences of NAO and Hudson Bay sea-ice on the climate of eastern Canada. *Climate Dynamics*, 31: 169–182, doi: http://dx.doi.org/10.1007/s00382-007-0343-9.

Saucier, F. J., and Dionne, J., 1998: A 3-D coupled ice-ocean model applied to Hudson Bay, Canada: the seasonal cycle and time-dependent climate response to atmospheric forcing and runoff. *Journal of Geophysical Research*, 103: 27689–27705.

Saucier, F. J., Senneville, S., Prinsenberg, S., Roy, F., Smith, G., Gachon, P., Caya, D., and Laprise, R., 2004: Modeling the ice-ocean seasonal cycle in Hudson Bay, Foxe Basin and Hudson Strait, Canada. *Climate Dynamics*, 23: 303–326, doi: http://dx.doi.org/10.1007/s00382-004-0445-6.

Stewart, B., and Barber, D. G., 2010: The ocean-sea ice-atmosphere system of the Hudson Bay Complex, *In* Stewart, S., Loseto, L., and Mallory, M. (eds.), *A Little Less Arctic: Top Predators in the World's Largest Inland Sea, Hudson Bay*. New York: Springer Verlag, 1–38.

St-Laurent, P., Straneo, F., Dumais, J. F., and Barber, D. G., 2011: What is the fate of the river waters of Hudson Bay? *Journal of Marine Systems*, 88: 352–361, doi: http://dx.doi.org/10.1016/j.jmarsys.2011.02.004.

Sutherland, D. A., Straneo, F., Lentz, S. J., and Saint-Laurent, P., 2011: Observations of fresh, anticyclonic eddies in the Hudson Strait outflow. *Journal of Marine Systems*, 88: 375–384, doi: http://dx.doi.org/10.1016/j.jmarsys.2010.12.004.

Vincent, L. A., and Gullett, D. W., 1999: Canadian historical and homogeneous temperature datasets for climate change analyses. *International Journal of Climatology*, 19: 1375–1388.

Vincent, L. A., Wang, X. L., Milewska, E. J., Wan, H., Yang, F., and Swail, V., 2012: A second generation of homogenized Canadian monthly surface air temperature for climate trend analysis. *Journal of Geophysical Research*, 117: D18110, doi: http://dx.doi.org/10.1029/2012JD017859.

Wang, J., Mysak, L. A., and Ingram, R. G., 1994: Interannual variability of sea-ice cover in Hudson Bay, Baffin Bay and the Labrador Sea. *Atmosphere-Ocean*, 32: 421–447.